Microchemical Journal 191 (2023) 108811

Contents lists available at ScienceDirect

Microchemical Journal

journal homepage: www.elsevier.com/locate/microc

Design and application of a smartphone-based device for in vineyard determination of anthocyanins content in red grapes

Camilla Menozzi [a,1], Rosalba Calvini [a,1], Giovanni Nigro [b], Paola Tessarin [b], Domenico Bossio [b], Marco Calderisi [c], Veronica Ferrari [a], Giorgia Foca [a], Alessandro Ulrici [a,*]

[a] Dipartimento di Scienze della Vita, Università di Modena e Reggio Emilia, Via Amendola, 2, 42122 Reggio Emilia, Italy
[b] Ri.Nova – Filiera Vitivinicola ed Olivo-Oleicola, Via Tebano 45, 48018 Faenza, Italy
[c] Kode Solutions, Lungarno Galileo Galilei, 1, 56125 Pisa, Italy

ARTICLE INFO

Keywords:
RGB imaging
Grape ripening
Multivariate image analysis
Anthocyanins
Smartphone

ABSTRACT

The choice of the proper moment for harvesting is a crucial aspect in winemaking process, since the chemical attributes of grape berries strongly influence red wine quality. In particular, phenolic composition of red grapes plays a significant role in many sensory properties of wine related to color and taste. Anthocyanins are the most important phenolic compounds for red grapes: they accumulate in the grape skin during ripening, and they are responsible for the purple color of ripe berries. Routine analysis for the determination of grapes phenolic maturity includes chromatographic and spectroscopic techniques, that are time-consuming and expensive. In this work, we propose an innovative device conceived for the determination of grape phenolic maturity based on RGB images of grape berries acquired with a smartphone. The device has been designed to be used directly in the vineyard thanks to its small size and to the possibility of acquiring geolocated images of the berries under controlled lighting conditions. In this study, grape samples of three different varieties (*Ancellotta*, *Lambrusco Salamino* and *Sangiovese*) were collected at different harvest times from veraison to maturity and imaged by means of a common smartphone using the device. The RGB images were then converted into one-dimensional signals, named colourgrams, which codify the color properties of the images. The dataset of colourgrams was then used to calculate calibration models using Partial Least Squares (PLS) regression in order to relate color information with chemical parameters generally employed to evaluate grape phenolic maturity, such as total anthocyanins content and extractable anthocyanins content. The calibration models were implemented in a software interface that allows to acquire geolocated images of the grape samples, visualize the outcomes of the analysis, visualize maps and plots related to phenolic maturity, store data and share relevant information.

1. Introduction

Grape harvesting at the optimal maturity stage is fundamental in wine production, since wine quality is strongly influenced by the amount of chemical compounds contained in the berries and the extractability of these compounds during the winemaking process [1,2]. The simple assessment of the so-called technological maturity, i.e., the ratio between sugars and acids content, is not sufficient to fully predict the oenological potential of grapes, since wine properties also depend on phenolic and aromatic maturity. Phenolic maturity refers to the potential of phenolic compounds, in particular anthocyanins present in grapes, while aromatic maturity corresponds to the maximum concentration of volatile compounds affecting wine aroma. Technological, phenolic and aromatic ripening processes have different behaviors and each one needs to be evaluated in order to properly assess oenological maturity of grapes and identify the optimal harvest time [3].

In particular, with regard to red grapes the concept of phenolic maturity has gained an increasing importance since it is related to the presence and abundance of phenolic compounds, which have a significant role in many sensory properties of red wines, like color stability, bitterness, astringency, body, and structure [3–8].

Anthocyanins are one of the most relevant groups of phenolic compounds. They are the red pigments in grapes which are responsible for the color of ripe berries and red wine [3,4,9–11]. The initial color of red

* Corresponding author.
E-mail address: alessandro.ulrici@unimore.it (A. Ulrici).
[1] These two authors equally contributed to this work.

https://doi.org/10.1016/j.microc.2023.108811
Received 21 December 2022; Received in revised form 7 April 2023; Accepted 25 April 2023
Available online 29 April 2023

wine is due predominantly to anthocyanins extracted from grape skin during crushing, pressing and fermentation, while final color depends on the formation of condensed pigments between free anthocyanins and colorless grape phenols, specifically, monomeric and polymeric flavanols (catechins and procyanidins), flavonols and phenolic acids during storage and ageing [11,12].

Anthocyanins gradually appear at veraison and accumulate primarily in the grape skin throughout the ripening process, while they tend to decrease during over-ripening [3,9]. Grapes do not ripen homogeneously and even each berry of the same bunch ripens at different rates due to multiple causes [8]. Indeed, different factors, like soil characteristics, climatic conditions, grape variety, agronomic practices and grape maturity level could affect the phenolic composition of grapes [7,11].

Furthermore, the ongoing climatic change is an aspect not to be neglected [13]. Unusual seasonal trends and extreme events are becoming increasingly frequent, and they have a significant impact on rural conditions. Consequently, the amount of phenolic compounds in red grapes could be heterogeneous even within the same physiological stage [14]. At the same time, having the optimal anthocyanins content at harvest time is important for wineries to obtain a quality product [6]. In this context, vineyards belonging to the same winery but located in different geographical positions require to be frequently inspected in order to monitor grape ripening and real-time feedbacks from the field are needed to make proper oenological choices.

Currently, qualitative and quantitative anthocyanins analysis is performed using chromatographic and spectroscopic techniques, which are time-consuming, invasive and expensive [15,16]. Indeed, these methods require a long and complex extraction procedure performed by trained personnel, and the use of dedicated laboratory instrumentation. For this reason, alternative approaches have been proposed with the aim of providing a rapid and comprehensive overview of the ripening process using non-destructive methods and portable devices [16–19]. Since the color of the berries is strongly related to the anthocyanins content, computer vision coupled with advanced techniques of image elaboration could be a rapid, non-destructive, cheap and environment-friendly alternative for the evaluation of phenolic maturity, thanks to the ease of use and flexibility of this tool [2].

More in general, RGB image analysis techniques have gained an increasing attention in the field of food analysis, since the progress in image acquisition technology has made nowadays possible a detailed non-destructive color evaluation even in case of matrices with heterogeneous aspect, like most of the food products [20–24]. Furthermore, one of the main advantages of computer vision systems consists in the possibility of acquiring RGB images of the considered samples using dedicated instrumentation as well as objects of common use such as digital cameras, flatbed scanners or smartphones.

The high complexity of RGB images data arrays makes essential to identify proper strategies for the extraction of the useful information, in particular when multiple images have to be simultaneously analyzed [24–27]. To solve this issue, the colourgrams approach has been successfully applied in several studies related to the analysis of food matrices by means of RGB imaging [20,21,28–33]. Colourgrams are one-dimensional signals codifying the color-related information of each RGB image and these signals can be analyzed by means of common multivariate analysis techniques [29,32]. In two recent papers, some of us successfully proposed the use of colourgrams, both alone and in combination with electrochemical signals, to quantitatively assess parameters related to grape ripening by analyzing grape must [33,34].

In the present study, we conceived a portable prototype in order to provide a fast and non-destructive support in the phenolic ripening assessment of grapes, by directly acquiring RGB images of grape berries using a common smartphone. The proposed system can be used directly in the vineyard with limited manipulation of the samples. The output of the analysis allows a quantitative determination of chemical parameters usually employed to assess phenolic ripening, i.e., total anthocyanins and extractable anthocyanins content. Furthermore, the use of a smartphone also allows to geolocate the images and share the results in real-time.

The prototype consists of a hardware for image acquisition (i.e., an acquisition box with a sample holder, illumination system and smartphone case) and proper software (smartphone app and web interface) for image elaboration and data storage. To our knowledge, this is the first time that RGB images of grape berries acquired with a smartphone are used to quantitatively estimate their anthocyanins content without any sample pretreatment.

In this work, grape samples of three different grape varieties (*Ancellotta*, *Lambrusco Salamino* and *Sangiovese*) were collected at different harvest times from veraison to maturity and imaged using the device. RGB images were converted into colourgrams and the dataset of colourgrams was used to build Partial Least Squares (PLS) calibration models to relate the color information of the images with the chemical parameters used to assess their anthocyanins content.

The following Materials and methods section is structured as follows: at first, we will describe hardware and software functionalities of the device, which was conceived to be as user-friendly as possible (*see* Section 2.1), and then we will describe in detail the development of all the data elaboration steps (*see* Sections 2.2–2.5) that are implemented in the software back-end. Finally, in the Results section (*see* Section 3) we will mainly focus on the calibration models obtained in the present study.

2. Materials and methods

2.1. The device

The device developed in this study to determine phenolic maturity of grape berries combines both hardware and software components. The hardware was designed to be compact in size and to enable the acquisition of grape samples images under controlled lighting conditions; in this manner it can be easily used by the winegrower directly in the vineyard. The software includes both a smartphone app and an interface accessible by a web browser, and it allows to acquire the geolocated images, display the results in real time, perform data sharing and storage.

2.1.1. The hardware

The hardware consists of an acquisition box of size 16 cm × 10 cm × 15.5 cm, a drawer used as sample holder and a sliding lid with a smartphone case (Fig. 1). All the hardware components were designed using the SketchUp software (Trimble) and printed with a 3D printer in black acrylonitrile–butadienestyrene (ABS). For image acquisition, the smartphone is placed inside its case in the sliding lid located in the upper part of the acquisition box, while the grape samples are placed in the sample holder. The smartphone used for this study was a Xiaomi Redmi Note 8 (Xiaomi, China), therefore the case was specifically designed based on the geometry (i.e., smartphone size and camera location) of this model.

A strip of white light emitting diode (LED) lights was fixed in the internal upper edge of the acquisition box, to ensure constant and homogeneous lighting conditions. The LED lights are powered by a power bank fixed outside the acquisition case, as shown in Fig. 1.

In addition, the lower inner part of the acquisition case contains a cardboard of color references, which are imaged with the sample and used for image correction (*see* Section 2.4.2).

2.1.2. The software

The dedicated software consists of a smartphone app and a web interface, which are connected to a web server where data are elaborated and stored.

Before providing a detailed description of the software features and for ease of comprehension, it is necessary to define some key terms/

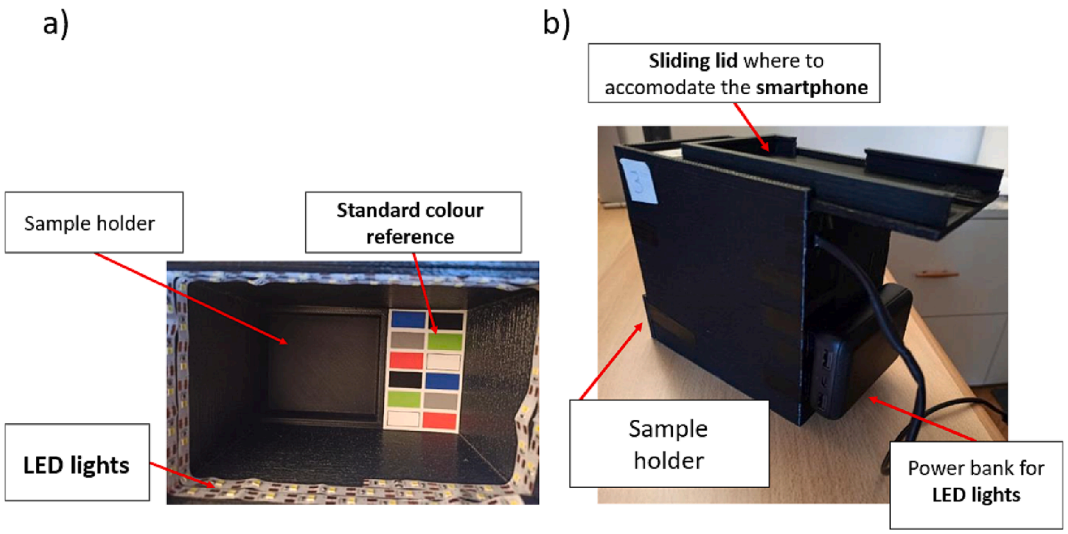

Fig. 1. Inner (a) and (b) outer structure of the acquisition device.

concepts, which will be used throughout the whole manuscript. In this work a *sample* consists of about 500 g of berries collected from different bunches located in different plants of the vineyard (*see* Section 2.2). For each sample, 6 *aliquots* were randomly collected (*see* Section 2.4.1) and a single *image* was acquired for each aliquot. Then, the 6 images corresponding to the 6 aliquots of each sample were merged together into a *scanset,* in order to better represent the intrinsic variability of the berries color within the considered sample (*see* Section 2.4.3). Therefore, a *scanset* is an image representation of a whole sample, while a single image represents an individual aliquot.

The smartphone app (Fig. 2) was designed to be used with ease, thanks to a friendly graphical user interface, which shows only the relevant information to the user.

From the left side of the screen an interactive list appears, where the user can select different menus (Fig. 2a). The "Scan" menu allows to acquire the geolocated images of the grape samples and to set additional sample information such as grape type and vineyard (Fig. 2b). According to the experimental procedure elaborated in this study (*see* Section 2.4), for each grape sample six different images of six aliquots of berries have to be acquired and then concatenated into a *scanset* for further elaboration. To make image acquisition as much user-friendly as possible, the smartphone app was developed to acquire and handle a *scanset* for each grape sample using the "Multiple Acquisition" mode. When using the "Multiple Acquisition" mode, the app displays the current *scanset* name, the currently acquired image number (between 1 and 6), and a preview of the acquired image to make it possible to decide whether to accept or discard it in case of a wrong acquisition (Fig. 2c).

Once acquired, the *scanset* is sent to the server together with the relevant metadata (geolocation, date and time) for image elaboration and storage, and the outcomes of the analysis can be displayed directly in the smartphone app using the "Analysis" menu. More in detail, as shown in Fig. 2d for each analyzed *scanset* it is possible to visualize sample name, time and date of acquisition, and the predicted content of the parameters of interest related to phenolic maturity: total

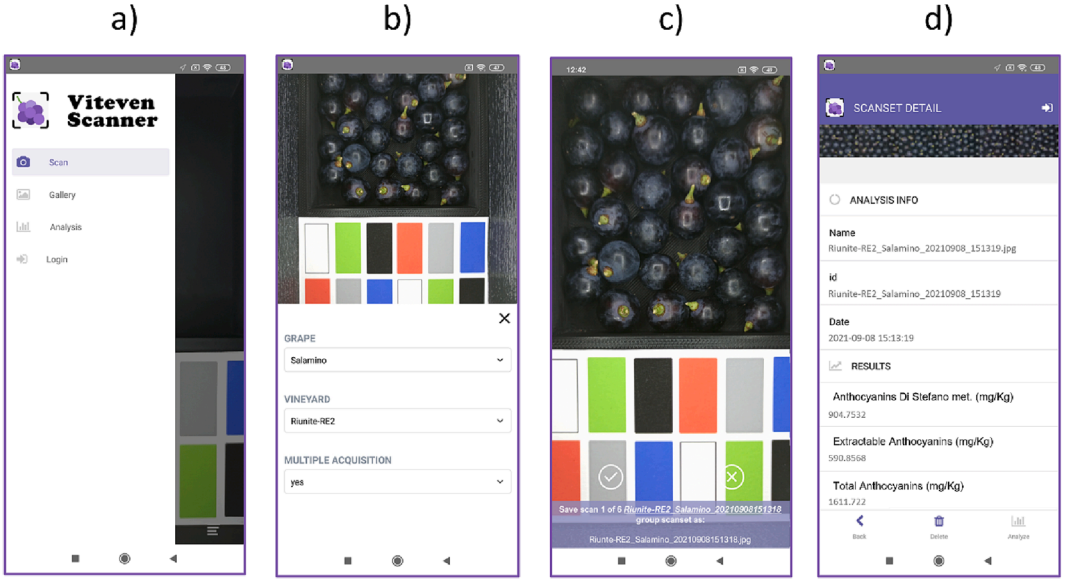

Fig. 2. Screenshots of the main features of smartphone app: a) selection of the "Scan" menu to acquire geolocated images of the grape samples; b) selection of the corresponding grape variety, vineyard and "Multiple Acquisition" mode to acquire the six images of a single sample that will be concatenated into a scanset; c) preview of the acquired image, with the possibility to discard or accept it; d) visualization of scanset details in the "Analysis" menu, showing sample name, time and date of acquisition, and predicted values of the parameters of interest for the selected scanset.

anthocyanins and extractable anthocyanins, both measured according to Glories method [35,36], and total anthocyanins measured according to Di Stefano method [37,38].

The web interface (Fig. 3) allows to access to the entire database of acquired images, considering also different grape varieties and different vineyards. In particular, it is possible to select a specific time range, one or more grape varieties and one or more vineyards, and visualize the corresponding results (Fig. 3a). The results are displayed as ripening maps, where each point corresponds to a *scanset* located in a specific geographical position (coded by the GPS coordinates of the *scanset*) and the point color indicates the corresponding value of the selected chemical parameter (Fig. 3b). In this manner, it is possible to easily evaluate the ripening stage of different parts of the same vineyard and/or of different vineyards. In addition, it is also possible to observe the ripening trend over the selected time period (Fig. 3c).

Finally, it is possible to select a specific sample in the ripening map, by clicking on the corresponding point, and visualize the corresponding *scanset* image together with the sample name, time and date of acquisition, and the predicted values of the chemical parameters (Fig. 3d).

Both smartphone app and web interface have been designed to be easily used by winegrowers to employ the proposed device to monitor grape phenolic maturity. Therefore, the whole data elaboration workflow that goes from image acquisition to the visualization of the outcomes of the analysis is automatically handled in back-end by server computing. In the following Sections (from Section 2.2 to Section 2.5) we will provide a detailed description of the procedure that we have followed to develop the multivariate calibration models implemented in the software.

2.2. Grape samples

To evaluate the effectiveness of the proposed device, three Italian purple grape varieties were considered: *Ancellotta* (A), *Lambrusco Salamino* (L) and *Sangiovese* (S), which correspond to the most common varieties used for wine production in Emilia-Romagna region (Italy).

The grape samples were harvested during vintages 2020 and 2021 in different vineyards located in the province of Reggio Emilia for *Ancellotta* and *Lambrusco Salamino* varieties, and in the province of Ravenna for *Sangiovese* variety. In particular, two vineyards were considered for each grape variety in vintage 2020, while three vineyards for each grape variety were considered in vintage 2021. In addition, the different vineyards considered for each grape variety were located both in hilly and flat areas in order to account for pedoclimatic variability.

For each variety and each vintage, grape samples were collected at subsequent harvest times, from veraison (30% of the berries of the bunches starting to change color) to complete ripening. In vintage 2020, a total of 8 harvest times were considered for *Ancellotta* and *Lambrusco Salamino* varieties, while 10 harvest times were considered for *Sangiovese* samples. Conversely, 10 subsequent harvest times were considered for all the three grape varieties in vintage 2021.

Each sample consisted of about 500 g of berries collected from different bunches located in different plants of the vineyard. The berries were collected in order to be as much representative as possible of vineyard variability of the ripening stage at the considered harvest time. Furthermore, the berries were collected paying attention to leave the fruit pedicel, in order to avoid the leakage of juice from the point of insertion.

RGB images of the collected samples were acquired using the device previously described in Section 2.1. In particular, for each sample six images of different randomly taken aliquots were acquired, in order to better represent the intrinsic variability of the berries color within each sample (*see* Section 2.4.1). More detailed information about the collected samples is reported in Table 1.

After harvesting, the collected grape samples were immediately carried to the laboratory under refrigerated conditions, where they were analyzed using the reference analytical methods that are commonly used by the wineries to determine the parameters of interest, i.e., total anthocyanins content (TAnt), extractable anthocyanins content (ExAnt) and total anthocyanins determined according to Di Stefano method (DS-TAnt).

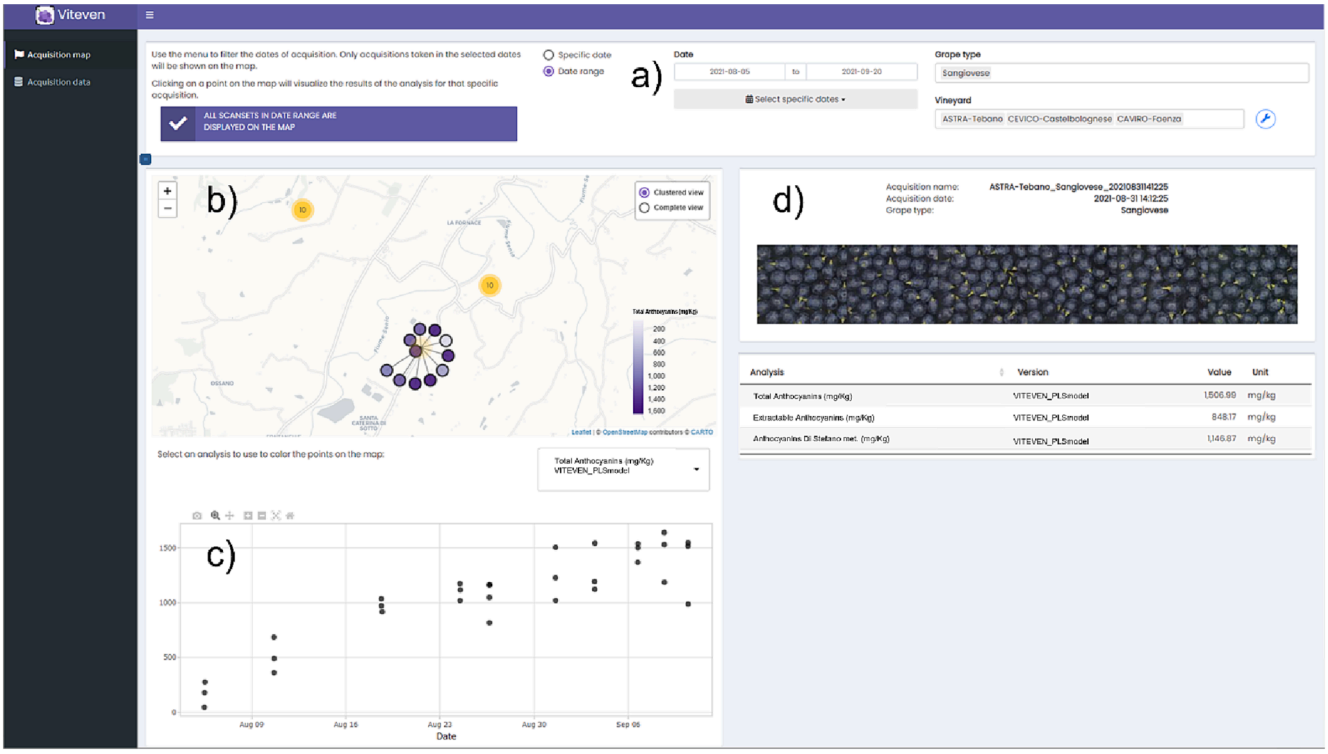

Fig. 3. Screenshot of the main features of the web interface: a) selection of date range, grape varieties and vineyards of interest; b) visualization of the ripening maps and c) ripening trend over the selected time period; d) visualization of a scanset image together with the predicted values of the chemical parameters.

Table 1
Information about the grape samples of the three grape varieties collected in 2020 and 2021 vintages.

Grape Variety	Year	Number of vineyards	Number of harvest times	Number of samples		Number of acquired images	
Ancellotta	2020	2	8	16	46	96	276
	2021	3	10	30		180	
zLambrusco Salamino	2020	2	8	16	46	96	276
	2021	3	10	30		180	
Sangiovese	2020	2	10	20	50	120	300
	2021	3	10	30		180	

2.3. Reference analysis for the determination of grape phenolic maturity

2.3.1. Total and extractable anthocyanins content

TAnt and ExAnt parameters were determined according to Glories method [35,36]. For each sample, grape berries were put in a blender (Kenwood CH-58) and mashed in order to homogenize pulp and skin. The so-obtained grape mash was divided into two aliquots of equal weight (Gibertini TM1600 Balance, Gibertini Elettronica, Milan, Italy): one aliquot was macerated in a pH 1 solution to have complete extraction of anthocyanins, while the second aliquot was macerated in a pH 3.2 solution to evaluate anthocyanins extractability at pH conditions similar to those of the winemaking process. After 4 h of maceration at room temperature under low agitation (BICASA BE39, BICASA srl, Monza Brianza, Italy), the two solutions were filtered on glass wool and spectrophotometric determination of anthocyanins (JASCO V-530, Tokyo, Japan) was performed on both clear juices using the methodology based on bleaching with sulfur dioxide [39–41]. The total anthocyanins content (TAnt, expressed as mg/Kg of malvidin-3-glucoside) and extractable anthocyanins content (ExtAnt, expressed as mg/Kg of malvidin-3-glucoside) were determined from the pH 1 and pH 3.2 solutions, respectively.

2.3.2. Total anthocyanins according to Di Stefano method

Total anthocyanins were also determined according to the method proposed by Di Stefano [37,38]. This method consists in measuring the content of anthocyanins present in the grape peel extracted in an alcoholic solution at pH of 3.2 and determined using spectrophotometric techniques. For each sample, grape berries were frozen in the shortest possible time and were immersed in a hydro-alcoholic buffer at pH of 3.2 containing tartaric acid, ethyl alcohol, sodium metabisulphite and sodium hydroxide. The berries where then homogenized with a Silverson homogenizer (SILVERSON Machine ltd, Chesham, UK) and the homogenate was subsequently centrifuged (ALC 3229 Centrifuge). The supernatant was then used for the spectrophotometric determination of anthocyanins (JASCO V-530, Tokyo, Japan). In particular, the concentration of total anthocyanins (expressed as mg/Kg of malvidin-3-glucoside) was calculated from the maximum absorbance value registered in the visible range, which falls at about 540 nm.

2.4. Image acquisition and elaboration

Fig. 4 provides a schematic representation of the different steps implemented in the device software from image acquisition of the grape samples to visualization of the predicted chemical parameters of interest related to phenolic ripening. These steps include:

1. Image acquisition using the smartphone app;
2. Image correction;
3. Concatenation of corrected sample images to create the *scansets*;
4. Conversion of *scansets* into colourgrams;
5. Prediction of chemical parameters by means of PLS models;
6. Display of the results on the smartphone app (and web interface).

In this study, the elaboration steps from image correction to the development and validation of the PLS models (steps 2–5) have been developed in MATLAB environment (The MathWorks Inc., USA) using both functions written *ad hoc* and the PLS Toolbox software (ver. 8.8.1, Eigenvector Research Inc., USA). Then, the corresponding algorithms and calibration models were implemented in the software so that the

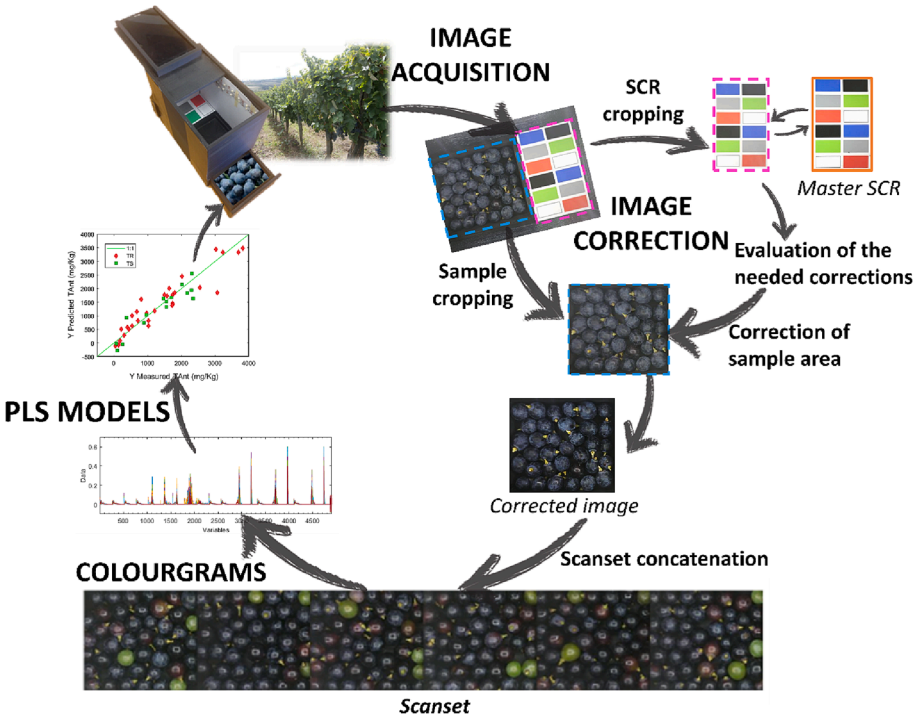

Fig. 4. From image acquisition of the grape samples to determination of anthocyanins content: main steps.

end user can simply acquire images and get the predictions with no further intervention needed.

All these steps are described in more detail in the following sections.

2.4.1. Image acquisition

For each sample, the collected berries were split into 6 aliquots and each aliquot was imaged using the device described in Section 2.1, equipped with a Xiaomi Redmi Note 8 smartphone embedding a 48 megapixels camera with a spatial resolution of 8000 × 6000 pixels, and considering a shutter speed of 1/50 s, f /1.9 lens aperture and ISO 200. The image scene also included a cardboard of standard color references used for the subsequent image standardization step. The RGB images were saved in JPEG file format with an average file size of 6 MB.

On the whole, 852 images were acquired, corresponding to 276 images for *Ancellotta* samples, 276 images for *Lambrusco Salamino* samples and 300 images for *Sangiovese* samples (*see* Table 1 for further details).

2.4.2. Image correction

A standardization procedure is highly recommended to reduce a possible variation among images, which can be caused by instrumental instability over time.

Each acquired image was composed by two different areas: the area with the cardboard of Standard Color References (SCR), that contains 12 colored rectangles, and the sample area with the grape berries. These two areas were automatically selected and cropped from the original image. The SCR area was then used to perform image standardization using the procedure previously described in detail by Orlandi et al., 2018 [33].

Basically, image correction consists in comparing the SCR of an image considered as reference (*master* image), usually the first acquired image, with the SCR of each one of the remainder images (*slave* images). If there are significant differences between the two references areas, the SCR of the slave image are corrected to be as much similar as possible to the SCR of the master image, and the same correction procedure is also applied to the whole slave image, including the sample area.

In particular, each one of the 12 color patches depicted in the color reference was divided into 4 pixels groups, according to a 2 × 2 grid. The median values of red (R), green (G) and blue (B) channels were calculated for each pixel group. These median values were subsequently stored in matrix of size {4 × 12, 3}, where 4 is the number of pixel groups, 12 is the number of the color reference patches and 3 corresponds to the R, G and B channels.

Then, an internal calibration was performed by computing, channel by channel, a regression model between the vector of median values of the master image (y) and the vector of median values of the i-th slave image (x_i). Based on some preliminary tests, a first-order polynomial was considered, which can be expressed as follows:

$$y(c) = b_0(i,c) + b_1(i,c) \times S_i(c) \quad (1)$$

where b_0 and b_1 are the regression coefficients calculated for the channel c of the i-th slave image, S_i. Furthermore, the algorithm also estimates the statistical significance of the model coefficients in order to select only the significant coefficients.

Then, the regression coefficients calculated as described above were used to correct each pixel of the corresponding sample area according to the following equation:

$$img_{corr}(i,c) = b_0(i,c) + b_1(i,c) \times img_{orig}(i,c) \quad (2)$$

where $img_{corr}(i,c)$ is the channel c of the i-th corrected image, $img_{orig}(i,c)$ is the channel c of the corresponding original image, and $b_0(i,c)$ and $b_1(i,c)$ are the model coefficients calculated using Equation (1).

Image correction was performed using RGB Correction GUI, a graphical user-friendly interface working under MATLAB (The MathWorks) environment and freely downloadable from https://www.chimslab.unimore.it/downloads/. The standardization procedure described above was also implemented in the software of the device in order to automatically correct the acquired images when necessary.

2.4.3. Conversion to colourgrams

After correction, the sample area of each image (i.e., the area containing the grape berries) was cropped obtaining a new image of size 2310 × 2623 pixels.

As mentioned in Section 2.1.2, each grape sample was randomly split into 6 aliquots that were separately imaged, thus obtaining 6 different images for each sample. However, for further analysis the corrected and cropped images of the 6 aliquots of the same sample were merged together into a *scanset*, therefore obtaining one merged image with size 2310 × 15,738 pixels for each sample. The dataset of merged sample images consisted therefore in 46 *scansets* for both *Ancellotta* and *Lambrusco Salamino* varieties, and in 50 *scansets* for *Sangiovese* variety.

This procedure was carried out in view of the development of the calibration models, where the determination of the chemical parameters was performed considering each sample as a whole and not considering the single aliquots. In addition, performing the evaluation considering more aliquots altogether allows to better account for sample variability and thus obtain more robust and reliable results.

Finally, each *scanset* was converted into the corresponding colourgram, a one-dimensional signal that codifies the color-related information content of the RGB image.

At first, *scanset* image is unfolded into a two-dimensional matrix with as many rows as the number of pixels and three columns corresponding to the R, G, and B channels [29].

Such 2D matrix is then expanded by adding new columns, corresponding to the following 16 additional parameters calculated from the R, G, B values for each image pixel:

- lightness (L), defined as the sum of R, G, B values;
- relative colors: relative Red (rR), relative Green (rG), relative Blue (rB), calculated as the ratio between each channel value and L;
- hue (H), saturation (S) and intensity (I), obtained by converting the RGB data into HSI color space;
- the three score vectors of the PCA model calculated from raw RGB data matrix (SC1R, SC2R, SC3R);
- the three score vectors of the PCA model calculated from mean centered RGB data matrix (SC1M, SC2M, SC3M);
- the three score vectors of the PCA model calculated from autoscaled RGB data matrix (SC1A, SC2A, SC3A).

Finally, the colourgram of each *scanset* is obtained by merging in sequence the frequency distribution curves of each one of the 19 considered color parameters (i.e., 3 RGB channels + 16 additional parameters). Each frequency distribution curve (i.e., a histogram with 256 bins) was calculated accounting for the entire range of variability of the considered parameter. In addition, at the end of the signal also the loading vectors and the eigenvalues of the three PCA models calculated on the RGB matrix are added, obtaining a 4900 points long signal. An example of the colourgrams obtained from the *scanset* images of *Sangiovese* samples is provided as Supplementary Material in Fig. S1. For a deeper insight of the algorithm developed to create the colourgrams, the reader is referred to Antonelli et al., 2004 and Calvini et al., 2020 [21,42].

Colourgrams are subsequently collected into a data matrix in which each row corresponds to the signal derived from a specific *scanset*, and such matrix can then be analyzed by means of common multivariate statistical methods for data exploration or for the development of regression models.

A preliminary evaluation of the colourgrams data matrix performed by means of PCA on mean centered signals allowed to observe that the correlation existing between the berry color and the corresponding anthocyanins content is specific for each single variety. For this reason, the

images obtained from the different grape varieties were analyzed separately from each other and three different matrices of colourgrams were obtained: one matrix with size {46 × 4900} for *Ancellotta* samples, one matrix with size {46 × 4900} for *Lambrusco Salamino* samples and one matrix with size {50 × 4900} for *Sangiovese* samples.

The colourgrams were calculated using Colourgrams GUI [42], a graphical user-friendly interface developed under MATLAB environment (The MathWorks Inc., USA) and freely downloadable from https://www.chimslab.unimore.it/downloads/. As for the standardization procedure, also the conversion of *scansets* into the corresponding colourgrams was implemented in the software of the device to be automatically performed.

2.5. Calculation of calibration models

Multivariate calibration models were calculated separately for each grape variety in order to predict the three chemical parameters of interest (**y** variables), i.e., total anthocyanins, extractable anthocyanins and total anthocyanins determined with Di Stefano method, using the colourgrams obtained from the *scansets* of the grape samples as predictors (**X** matrix).

To this aim, each one of the three colourgram matrices, corresponding to the three grape varieties, was split into a training set and a test set. The subdivision of the samples between training and test sets was done in a way to attribute to the test set different harvest times for each vineyard. The training set was used to calculate the calibration models using Partial Least Squares regression [43,44], while the test set was used to perform an external validation of the obtained models. In particular, for both *Ancellotta* and *Lambrusco Salamino* colourgrams matrices 31 signals were considered in the training set and 15 signals were considered in the test set. Conversely, for *Sangiovese* colourgrams matrix, one sample was detected as outlier and the remainder samples were split into training and test sets as follows: 34 signals in the training set and 15 signals in the test set.

For the calculation of the PLS models, the colourgrams matrices were preprocessed using mean center, and the optimal number of Latent Variables (LVs) was selected by minimizing the Root Mean Square Error in Cross-Validation (RMSECV), considering a venetian blinds cross-validation scheme with 5 deletion groups.

The performance of the calibration models was expressed in terms of Root Mean Square Error (RMSE) and coefficient of determination (R^2) statistics, both calculated in calibration (RMSEC, R^2_{Cal}), cross-validation (RMSECV, R^2_{CV}) and prediction (RMSEP, R^2_P). The PLS models were calculated using the PLS Toolbox (ver. 8.8.1, Eigenvector Research Inc., USA) running under MATLAB environment (The Mathworks Inc., USA). The calibration models developed in this study were then implemented in the software architecture of the device.

As mentioned in Section 2.4.3, the PLS models implemented into the device were calculated separately for each grape variety, since for each variety a specific relationship between berries color and anthocyanins content was observed. This behavior is likely ascribable to the peculiar physiology and ripening behavior of each plant variety. However, for the sake of completeness, we also calculated global PLS models, i.e., considering the entire set of samples of the three varieties altogether.

3. Results and discussion

3.1. Evaluation of the chemical parameters related to phenolic maturity

In this work, the calibration models were calculated considering grape samples belonging to different grape varieties and harvested in three different vineyards. In particular, in the case of *Ancellotta* and *Lambrusco Salamino* varieties, one vineyard was located in hilly areas while the other two vineyards were located in flat areas. Conversely, for *Sangiovese* variety two vineyards were located in hilly areas and one vineyard was located in a flat area.

The different geographical position of the vineyards is a relevant aspect to be considered for the development of the calibration models, since the differences in pedoclimatic conditions can affect the grape ripening trend. In this context, we observed some differences in the ripening trends between vineyards with different geographical position. For example, Fig. 5 shows the trends of total anthocyanins content for the three varieties in 2020 and 2021 vintage years according to the different vineyards. In the case of *Lambrusco Salamino* variety, it is particularly evident that the samples harvested in the vineyard located in a foot-hill region (Sal-B) tend to reach a higher anthocyanins amount compared to samples harvested in the vineyards located in flat areas (Sal-A and Sal-C). Similar results were also obtained considering *Ancellotta* samples. As shown in Fig. 5, for *Sangiovese* variety the variability among vineyards located in different geographical positions is less evident compared to the other grape varieties; this could be due to the fact that, compared with the vineyards of *Ancellotta* and *Lambrusco Salamino*, for *Sangiovese* variety the vineyards located in hilly areas were much closer to those located in flat areas.

Similar trends were also observed considering the evolution of ExAnt and DSAnt trends over time for the three grape varieties (Figs. S2 and S3 of Supplementary Material).

For a more comprehensive evaluation of the oenological characteristics of the collected samples, Figs. S4-S6 of Supplementary Material report the box plots of TAnt, ExAnt and DSAnt grouped according to grape varieties for both 2020 and 2021 vintage years. It is possible to observe that *Ancellotta* samples reach higher values for all the three parameters, while *Sangiovese* variety is generally characterized by a lower anthocyanins content with respect to *Ancellotta* and *Lambrusco Salamino* varieties. Considering vintage years, the differences are more evident considering TAnt parameter and *Ancellotta* samples, indeed in 2021 the total anthocyanins content for this grape variety reached higher values compared to 2020 vintage year.

3.2. PLS models

Before the calculation of the PLS models, a preliminary exploratory analysis was performed by means of PCA considering the colourgrams of the images acquired from the samples belonging to all the three grape varieties. The corresponding PC1 and PC2 score plot is reported in Fig. S7 of Supplementary Material, where the samples are colored according to grape variety (Fig. S7a), vintage year (Fig. S7b), vineyard location (Fig. S7c) and harvest day (Fig. S7d). It is possible to observe that PC1 mainly describes the color evolution of grape samples during ripening and that the samples belonging to the different varieties follow different ripening trends. *Ancellotta* samples are generally located at higher PC1 score values, suggesting that this variety has a more pronounced color variation during ripening. To better evaluate the relationship between the color of the berries and total anthocyanins content, Fig. S8 of Supplementary Material shows the plot of TAnt values *vs.* PC1 scores of the global PCA model calculated considering the colourgrams of the samples belonging to the three grape varieties. It is evident that each grape variety has a peculiar ripening trend and that a similar color of the berries may correspond to a very different TAnt value.

In order to relate the color information contained in the RGB images of grape samples with the corresponding parameters of interest to estimate phenolic maturity, a total of 9 PLS1 models (=3 grape varieties × 3 chemical parameters) were calculated using the colourgrams approach. In particular, as shown from the global PCA results discussed above, each grape variety has a peculiar maturation trend, therefore it is necessary to calculate separate calibration models for each grape variety. The results of the corresponding PLS models are reported in Table 2.

Generally, for all the three grape varieties the best results were obtained in the prediction of the total anthocyanins content (TAnt), with R^2_P values equal to 0.60, 0.85 and 0.81 for *Ancellotta*, *Lambrusco Salamino* and *Sangiovese*, respectively. For both *Lambrusco Salamino* and *Sangiovese* varieties the calibration models for the prediction of extractable

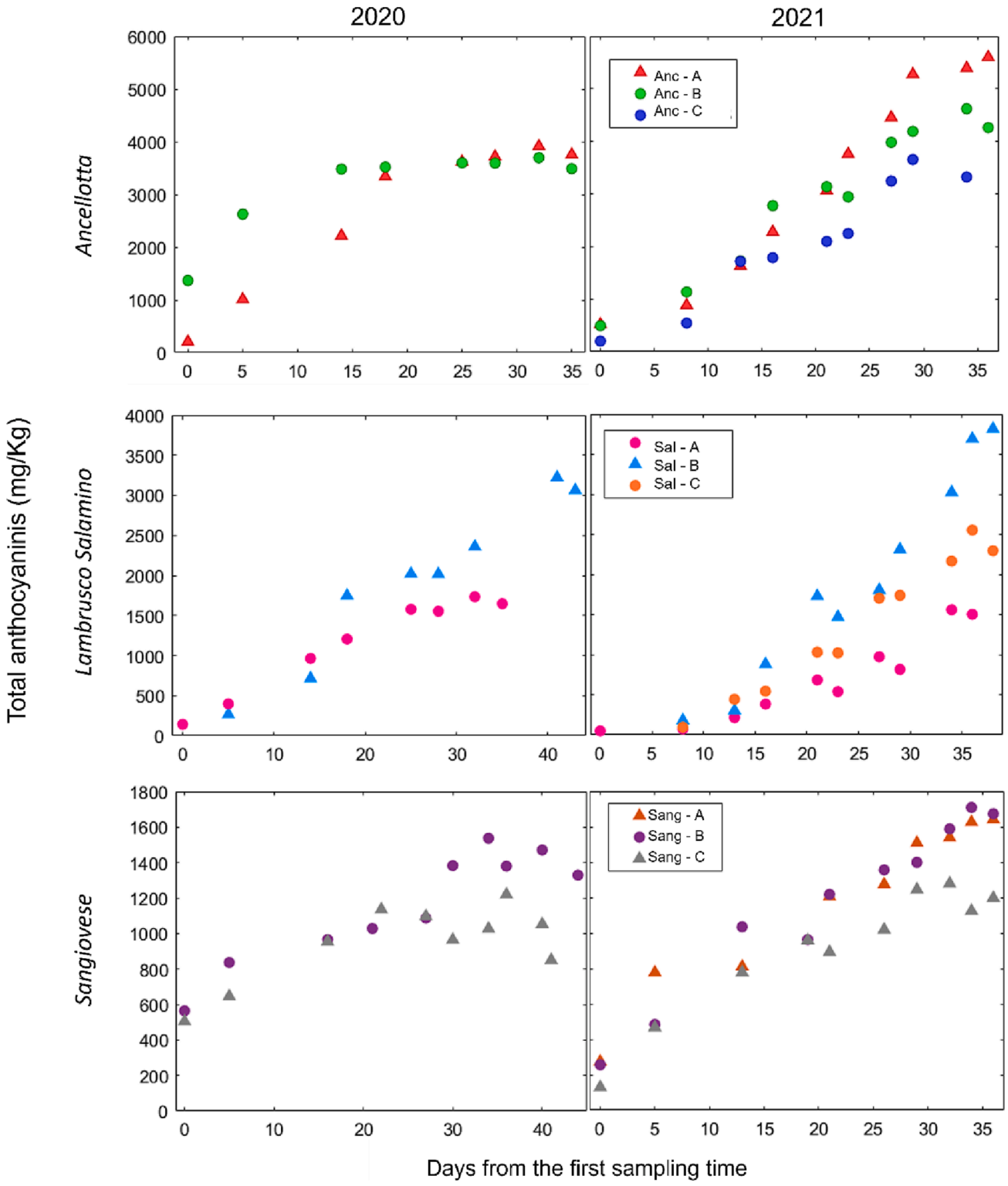

Fig. 5. Total anthocyanins trends for Ancellotta, Lambrusco Salamino and Sangiovese in 2020 and 2021 vintages; samples are colored according to the corresponding vineyard; triangles are referred to vineyards located in hilly areas, while circles to vineyards located in flat areas.

anthocyanins content led to similar or slightly lower results compared to those obtained for TAnt, while for *Ancellotta* variety ExAnt provided lower prediction results and DSAnt model performed better.

Comparing the model performances obtained for the three grape varieties, the overall best results for all the three phenolic ripening parameters were obtained for *Lambrusco Salamino* variety followed by *Sangiovese* variety, with R^2_P values higher than 0.81 and 0.71, respectively. In general, for these two varieties the obtained results can be considered very satisfactory, in view of the practical application of the device. Indeed, the possibility of an extensive and frequent sampling to get information in real-time about grape ripening, although with lower precision, is preferrable compared to using only the reference analytical methods. In fact, the latter require to send the samples to specialized analytical laboratories, which implies a significant time

Table 2
Results of the PLS models.

Grape Variety	Y Variable	LVs	RMSEC	RMSECV	RMSEP	R^2_{Cal}	R^2_{CV}	R^2_P
Ancellotta	TAnt	2	710	821	867	0.76	0.67	0.60
	ExAnt	1	346	382	427	0.70	0.64	0.51
	DSAnt	1	524	567	653	0.74	0.69	0.58
Lambrusco Salamino	TAnt	2	374	465	314	0.88	0.81	0.85
	ExAnt	2	159	188	137	0.87	0.81	0.85
	DSAnt	2	258	322	233	0.86	0.79	0.81
Sangiovese	TAnt	4	100	144	158	0.94	0.87	0.81
	ExAnt	4	71	95	103	0.91	0.83	0.77
	DSAnt	4	97	149	137	0.90	0.76	0.71

delay between sampling and obtaining the analysis result; moreover, this also drastically limits the number of determinations that can be done during grape ripening.

Fig. 6 reports the measured values *vs.* the predicted values of the PLS models calculated for TAnt parameter for all the three grape varieties (the same plots for ExAnt and DSAnt are reported as supplementary material in Figs. S9 and S10). These plots confirm the satisfactory calibration performances obtained for both *Lambrusco Salamino* and *Sangiovese* varieties; indeed, the samples are generally close to the bisector.

Conversely, for *Ancellotta* grape variety the calibration models (Table 2) led to not fully satisfactory results: the R^2 values calculated in cross-validation (R^2_{CV}) were between 0.64 and 0.69, while in prediction the R^2 values (R^2_P) were between 0.51 and 0.60.

Observing the plots of the measured TAnt values *vs.* the predicted values obtained for the PLS model of *Ancellotta* variety reported in Fig. 6, it is possible to understand the reason behind the low performances obtained for this grape variety. As a matter of fact, the samples with measured TAnt values lower than 2000 mg/Kg are close to the bisector, thus correctly predicted by the model. Conversely, the samples with measured TAnt values higher than 2000 mg/Kg are all predicted with values falling in the range 2500 – 4500 mg/Kg but with low accordance with the corresponding values determined with the reference analytical methods. In particular, the samples with actual TAnt values between 2000 mg/Kg and 3000 mg/Kg tend to be overestimated, while those samples with actual TAnt values higher than 4000 mg/Kg tend to be underestimated. These findings suggest that for *Ancellotta* variety at high TAnt values there is a low correlation between the color of the berries and the total amount of anthocyanins. As a matter of fact, *Ancellotta* variety has a peculiar behavior compared to the other grape varieties considered in this study: *Ancellotta* berries tend to change color and become totally dark violet at the beginning of the maturation even if the ripening phenomena continue to evolve, also including the increase of anthocyanins content. In fact, compared to the other red grape varieties commonly used in Emilia Romagna region (Italy), *Ancellotta* is characterized by a high concentration of anthocyanins in the skin of the berries leading to their strong pigmentation, which makes this variety ideal as a colorant for red wines. A similar ripening behavior was also observed in previous studies for other grape varieties such as *Tempranillo* and *Syrah* [11]. A possible solution to overcome this limitation could be the acquisition of overexposed images of ripe berries, in order to better

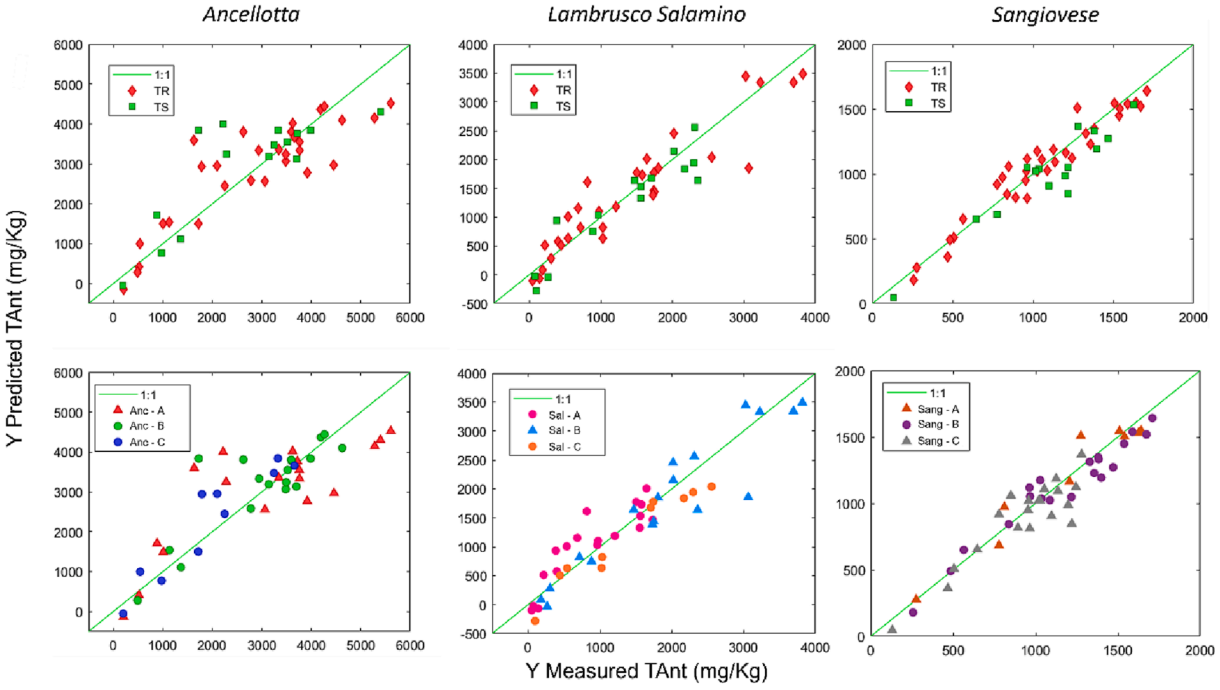

Fig. 6. Experimentally measured amount of total anthocyanins content (TAnt, expressed as mg/Kg of malvidin-3-glucoside) *vs.* predicted amount of the PLS models calculated for Ancellotta, Lambrusco Salamino and Sangiovese varieties. For each model, in the upper part of the figure the samples are colored according to training (TR) and test (TS) sets, while on the lower part of the figure the samples are colored according to the corresponding vineyard; triangles are referred to vineyards located in hilly areas, while circles to vineyards located in flat areas.

detect subtle color changes that are hardly distinguishable at the naked eye when the berries color is dark purple.

Another factor that could negatively affect the prediction models is the presence of grape bloom, a waxy compound of white color that covers the berries. In this study, the grape samples were imaged without a prior removal of grape bloom to minimize their manipulation and, thus, to facilitate the use of the device directly in the vineyard. However, for grape varieties with peculiar ripening trends such as *Ancellotta*, the removal of the grape bloom from the berries prior to image acquisition could help in removing non-informative variability sources and to improve the results of the calibration models.

Finally, in order to evaluate the color parameters included in the colourgrams that are more relevant for the calibration models, the Variable Importance in Projection (VIP) scores were considered. As a general rule, variables with VIP score values greater than one are assumed to provide a substantial contribution to the corresponding model.

A comparison of the VIP scores of the three models for TAnt (available in Figs. S11-S13 of Supplementary Material) shows that the most important variables, even if not precisely overlapping, always correspond to the same colourgram parameters for every variety. The colourgrams intervals arising as significant fall in the regions corresponding to the relative colors (rR, rG and rB), hue (H), the score vectors of PC2 and PC3 applied to both raw (SC2 R, SC3 R), mean centered (SC2 M, SC3 M) and autoscaled (SC2 A, SC3 A) RGB data matrix and a portion the loadings, which slightly diverges between the three models.

The same color parameters were observed as significant also considering the VIP scores of the PLS models calculated to predict ExAnt and DSAnt for all the varieties (Figs. S11-S13 of Supplementary Material).

For the sake of completeness, also global PLS models were calculated, considering all the three grape varieties altogether. However, the corresponding results were much lower than those obtained for the PLS models specific for each variety (Table S1 and Figs. S14-S16 of Supplementary Material). As discussed above, *Ancellotta* samples have a very peculiar ripening trend which is different from the behavior of the samples of the other varieties, therefore we also calculated PLS models considering only the *Lambrusco Salamino* and *Sangiovese* samples altogether (Table S2 and Figs. S17-S19). However, also in this case the model performances resulted much lower than those of the PLS models calculated for each single variety. These findings further confirmed that the relationship between color of the berries and anthocyanins profile is peculiar for each grape variety, therefore it is necessary to model such relationship considering specific PLS models for each considered variety.

4. Conclusions

In the present study, we discussed the design and application of a portable device conceived to be a fast and user-friendly tool to support winegrowers in the assessment of anthocyanins content of red grapes directly in the vineyard. The hardware part of the device is composed of a portable acquisition box that allows to acquire RGB images of the grape samples under controlled lighting conditions using a smartphone. The core idea behind the device consists in relating the color information of the grape samples contained in RGB images with the chemical parameters of interest using a data dimensionality reduction algorithm and multivariate calibration. All the data elaboration steps required to obtain the final prediction of the parameters of interest starting from the RGB images of the grape samples were implemented in the user-friendly software interface of the device. Through this software interface, the end user can easily acquire geolocated images of grape samples, view and share the results of the analysis in real time, without the need for any particular skills other than to carry out correct sampling.

In the phase of development and validation of the calibration models that have been implemented in the device, satisfactory results were obtained in the prediction of the chemical parameters of interest for the assessment of grape phenolic maturity of *Lambrusco Salamino* and *Sangiovese* varieties. Compared to the traditional methods used to evaluate grape phenolic ripening, the proposed device offers the possibility to perform much more frequent measurements and to get information in real-time about grape ripening. Furthermore, it must be considered that traditional analytical methods are quite expensive and time consuming, since they require a laborious sample preparation step to extract anthocyanins from the skin of grape berries. In addition, also these reference analytical methods are affected by a significant degree of uncertainty due to the low stability of the extracted grape must.

Conversely, lower calibration performances were obtained for *Ancellotta* grape variety, probably due to its exceptionally high concentration of anthocyanins in the skin of the berries. To improve the prediction performances for grape varieties with an early color change and particularly high anthocyanin contents, like *Ancellotta*, it will be necessary to optimize *ad hoc* the conditions for image acquisition.

In general, in order to further increase the robustness of the calibration models, it will be necessary to acquire a larger number of samples, and to consider both the application of variable selection algorithms and the possibility of developing local models for specific vineyards or restricted geographic areas.

The proposed device provides winegrowers and all the stakeholders (like, e.g., winemakers) with relevant information about grape ripening in real-time, allowing to support a proper planning of the optimal harvest time and the organization of the entire winemaking process. In fact, it is possible not only to monitor time evolution and spatial variability of the parameters of interest, but also to make comparisons with stored data of previous vintages. In this manner, it is possible to have a real-time screening of grape phenolic ripening in a specific vineyard and move to laboratory analysis only if necessary.

For a practical application of the proposed device, it must be taken into account the possible variability due to the acquisition of the images using different smartphone models. In this regard, the standardization procedure described in this study could be helpful to minimize color variations and ensure the stability of the prediction models. In addition, it is also possible to consider the use of calibration transfer strategies, which are commonly used in Near Infrared (NIR) spectroscopy applications to transfer the calibration models from different devices. These aspects will be evaluated in future studies.

CRediT authorship contribution statement

Camilla Menozzi: Methodology, Software, Formal analysis, Validation, Investigation, Data curation, Writing – original draft, Writing – review & editing. **Rosalba Calvini:** Methodology, Software, Formal analysis, Validation, Investigation, Data curation, Writing – original draft, Writing – review & editing. **Giovanni Nigro:** Project administration, Funding acquisition, Resources, Writing – review & editing. **Paola Tessarin:** Resources, Investigation, Writing – review & editing. **Domenico Bossio:** Resources, Investigation, Writing – review & editing. **Marco Calderisi:** Software, Data curation, Resources, Visualization, Writing – review & editing. **Veronica Ferrari:** Investigation, Writing – review & editing. **Giorgia Foca:** Investigation, Writing – review & editing. **Alessandro Ulrici:** Conceptualization, Methodology, Validation, Investigation, Writing – review & editing, Supervision, Project administration, Funding acquisition.

Declaration of Competing Interest

The authors declare the following financial interests/personal relationships which may be considered as potential competing interests: Alessandro Ulrici has patent #Italian Patent 102,018,000,004,498 issued to UNIVERSITA' DEGLI STUDI DI MODENA E REGGIO EMILIA.

Data availability

Data will be made available on request.

Acknowledgements

The present study was carried out in the frame of the Regional Rural Development Program 2014–2020 - Type of Operation 16.1.01 - Operational Groups of the European Innovation Partnership: "Agricultural productivity and sustainability" Focus Area 3A - Project "Technological innovation for efficient harvest forecasting - VITEVEN" (Programma Regionale di Sviluppo Rurale 2014–2020 – Tipo di Operazione 16.1.01 – Gruppi operativi del Partenariato Europeo per l'Innovazione: "produttività e sostenibilità dell'agricoltura" Focus Area 3A – Progetto "Innovazione tecnologica per una efficiente previsione vendemmiale - VITEVEN", CUP E48H19000830005).

Rosalba Calvini would like to thank the Italian funding programme *Fondo Sociale Europeo REACT-EU - PON "Ricerca e Innovazione" 2014 – 2020 – Azione IV.6 Contratti di ricerca su tematiche Green (D.M. 1062 del 10/08/ 2021)* for supporting her research (CUP: E95F21002330001; contract number 17-G-13884–4).

The authors wish also to thank the team of KODE Solutions for the development of the software interface of the device and Dr. Paolo Piscolla (ASTRA) for the support with reference analyses on grape samples.

Appendix A. Supplementary data

Supplementary data to this article can be found online at https://doi.org/10.1016/j.microc.2023.108811.

References

[1] A.B. Bautista-Ortín, J.I. Fernández-Fernández, J.M. López-Roca, E. Gómez-Plaza, The effect of grape ripening stage on red wine color, OENO One 40 (2006) 15. https://doi.org/10.20870/oeno-one.2006.40.1.879.

[2] E. Vrochidou, C. Bazinas, G.A. Papakostas, T. Pachidis, V.G. Kaburlasos, A review of the state-of-art, limitations, and perspectives of machine vision for grape ripening estimation, Engineering Proceedings 9 (2021) 2, https://doi.org/10.3390/engproc2021009002.

[3] P. Ribéreau-Gayon, D. Dubourdieu, B. Donèche, Handbook of enology, 2nd ed,, John Wiley, Chichester, West Sussex, England; Hoboken, NJ, 2006.

[4] E. García-Beneytez, E. Revilla, F. Cabello, Anthocyanin pattern of several red grape cultivars and wines made from them, Eur. Food Res. Technol. 215 (2002) 32–37, https://doi.org/10.1007/s00217-002-0526-x.

[5] S. Pérez-Magariño, M.L. González-San José, Polyphenols and colour variability of red wines made from grapes harvested at different ripeness grade, Food Chem. 96 (2006) 197–208, https://doi.org/10.1016/j.foodchem.2005.02.021.

[6] S. Chen, F. Zhang, J. Ning, X. Liu, Z. Zhang, S. Yang, Predicting the anthocyanin content of wine grapes by NIR hyperspectral imaging, Food Chem. 172 (2015) 788–793, https://doi.org/10.1016/j.foodchem.2014.09.119.

[7] S. Pérez-Magariño, M.L. González-San José, Evolution of flavanols, anthocyanins, and their derivatives during the aging of red wines elaborated from grapes harvested at different stages of ripening, J. Agric. Food Chem. 52 (2004) 1181–1189, https://doi.org/10.1021/jf035099i.

[8] N. Kontoudakis, M. Esteruelas, F. Fort, J.M. Canals, V. De Freitas, F. Zamora, Influence of the heterogeneity of grape phenolic maturity on wine composition and quality, Food Chem. 124 (2011) 767–774, https://doi.org/10.1016/j.foodchem.2010.06.093.

[9] J.A. Kennedy, M.A. Matthews, A.L. Waterhouse, Effect of maturity and vine water status on grape skin and wine flavonoids, Am J Enol Vitic 53 (4) (2002) 268–274.

[10] F. Mattivi, C. Zulian, G. Nicolini, L. Valenti, Wine, Biodiversity, Technology, and Antioxidants, Ann. N. Y. Acad. Sci. 957 (2002) 37–56, https://doi.org/10.1111/j.1749-6632.2002.tb02904.x.

[11] F.J. Rodríguez-Pulido, A.B. Mora-Garrido, M.L. González-Miret, F.J. Heredia, Research Progress in Imaging Technology for Assessing Quality in Wine Grapes and Seeds, Foods 11 (2022) 254, https://doi.org/10.3390/foods11030254.

[12] M. Garciafalcon, C. Perezlamela, E. Martinezcarballo, J. Simalgandara, Determination of phenolic compounds in wines: Influence of bottle storage of young red wines on their evolution, Food Chem. 105 (2007) 248–259, https://doi.org/10.1016/j.foodchem.2006.11.006.

[13] J. Drappier, C. Thibon, A. Rabot, L. Geny-Denis, Relationship between wine composition and temperature: Impact on Bordeaux wine typicity in the context of global warming—Review, Crit. Rev. Food Sci. Nutr. 59 (2019) 14–30, https://doi.org/10.1080/10408398.2017.1355776.

[14] J. Nogales-Bueno, B. Baca-Bocanegra, F.J. Rodríguez-Pulido, F.J. Heredia, J. M. Hernández-Hierro, Use of near infrared hyperspectral tools for the screening of extractable polyphenols in red grape skins, Food Chem. 172 (2015) 559–564, https://doi.org/10.1016/j.foodchem.2014.09.112.

[15] S. Gutiérrez, J. Tardaguila, J. Fernández-Novales, M.P. Diago, On-the-go hyperspectral imaging for the in-field estimation of grape berry soluble solids and anthocyanin concentration: Hyperspectral imaging for in-field grape estimation, Australian Journal of Grape and Wine, Research 25 (2019) 127–133, https://doi.org/10.1111/ajgw.12376.

[16] A. Ribera-Fonseca, M. Noferini, E. Jorquera-Fontena, A.D. Rombolà, Assessment of technological maturity parameters and anthocyanins in berries of cv. Sangiovese (Vitis vinifera L.) by a portable vis/NIR device, Sci. Hortic. 209 (2016) 229–235, https://doi.org/10.1016/j.scienta.2016.06.004.

[17] B. Baca-Bocanegra, J.M. Hernández-Hierro, J. Nogales-Bueno, F.J. Heredia, Feasibility study on the use of a portable micro near infrared spectroscopy device for the "in vineyard" screening of extractable polyphenols in red grape skins, Talanta 192 (2019) 353–359, https://doi.org/10.1016/j.talanta.2018.09.057.

[18] D. dos Santos Costa, N.F. Oliveros Mesa, M. Santos Freire, R. Pereira Ramos, B. J. Teruel Mederos, Development of predictive models for quality and maturation stage attributes of wine grapes using vis–nir reflectance spectroscopy, Postharvest Biol. Technol. 150 (2019) 166–178, https://doi.org/10.1016/j.postharvbio.2018.12.010.

[19] A. Pampuri, A. Tugnolo, V. Giovenzana, A. Casson, R. Guidetti, R. Beghi, Design of cost-effective LED based prototypes for the evaluation of grape (Vitis vinifera L.) ripeness, Comput. Electron. Agric. 189 (2021), 106381, https://doi.org/10.1016/j.compag.2021.106381.

[20] A. Ulrici, G. Foca, M.C. Ielo, L.A. Volpelli, D.P. Lo Fiego, Automated identification and visualization of food defects using RGB imaging: Application to the detection of red skin defect of raw hams, Innov. Food Sci. Emerg. Technol. 16 (2012) 417–426, https://doi.org/10.1016/j.ifset.2012.09.008.

[21] A. Antonelli, M. Cocchi, P. Fava, G. Foca, G.C. Franchini, D. Manzini, A. Ulrici, Automated evaluation of food colour by means of multivariate image analysis coupled to a wavelet-based classification algorithm, Anal. Chim. Acta 515 (2004) 3–13, https://doi.org/10.1016/j.aca.2004.01.005.

[22] T. Brosnan, D.-W. Sun, Improving quality inspection of food products by computer vision—a review, J. Food Eng. 61 (2004) 3–16, https://doi.org/10.1016/S0260-8774(03)00183-3.

[23] T. Brosnan, D.-W. Sun, Inspection and grading of agricultural and food products by computer vision systems—a review, Comput. Electron. Agric. 36 (2002) 193–213, https://doi.org/10.1016/S0168-1699(02)00101-1.

[24] R. Calvini, L. Pigani, Toward the Development of Combined Artificial Sensing Systems for Food Quality Evaluation: A Review on the Application of Data Fusion of Electronic Noses, Electronic Tongues and Electronic Eyes, Sensors 22 (2022) 577, https://doi.org/10.3390/s22020577.

[25] J.M. Prats-Montalbán, A. de Juan, A. Ferrer, Multivariate image analysis: A review with applications, Chemom. Intel. Lab. Syst. 107 (2011) 1–23, https://doi.org/10.1016/j.chemolab.2011.03.002.

[26] J.M. Prats-Montalbán, A. Ferrer, Integration of colour and textural information in multivariate image analysis: defect detection and classification issues, J. Chemometr. 21 (2007) 10–23, https://doi.org/10.1002/cem.1026.

[27] P.H. Gonçalves Dias Diniz, Chemometrics-assisted color histogram-based analytical systems, J. Chemom. 34 (2020), https://doi.org/10.1002/cem.3242.

[28] G. Orlandi, R. Calvini, G. Foca, A. Ulrici, Automated quantification of defective maize kernels by means of multivariate image analysis, Food Control 85 (2018) 259–268, https://doi.org/10.1016/j.foodcont.2017.10.008.

[29] A. Giraudo, R. Calvini, G. Orlandi, A. Ulrici, F. Geobaldo, F. Savorani, Development of an automated method for the identification of defective hazelnuts based on RGB image analysis and colourgrams, Food Control 94 (2018) 233–240, https://doi.org/10.1016/j.foodcont.2018.07.018.

[30] A. Borin, M.F. Ferrão, C. Mello, L. Cordi, L.C.M. Pataca, N. Durán, R.J. Poppi, Quantification of Lactobacillus in fermented milk by multivariate image analysis with least-squares support-vector machines, Anal. Bioanal. Chem. 387 (2007) 1105–1112, https://doi.org/10.1007/s00216-006-0971-7.

[31] M. Corti, D. Cavalli, G. Cabassi, A. Vigoni, L. Degano, P. Marino Gallina, Application of a low-cost camera on a UAV to estimate maize nitrogen-related variables, Precision Agric. 20 (2019) 675–696, https://doi.org/10.1007/s11119-018-9609-y.

[32] G. Foca, F. Masino, A. Antonelli, A. Ulrici, Prediction of compositional and sensory characteristics using RGB digital images and multivariate calibration techniques, Anal. Chim. Acta 706 (2011) 238–245, https://doi.org/10.1016/j.aca.2011.08.046.

[33] G. Orlandi, R. Calvini, L. Pigani, G. Foca, G. Vasile Simone, A. Antonelli, A. Ulrici, Electronic eye for the prediction of parameters related to grape ripening, Talanta 186 (2018) 381–388, https://doi.org/10.1016/j.talanta.2018.04.076.

[34] G. Orlandi, R. Calvini, G. Foca, L. Pigani, G. Vasile Simone, A. Ulrici, Data fusion of electronic eye and electronic tongue signals to monitor grape ripening, Talanta 195 (2019) 181–189, https://doi.org/10.1016/j.talanta.2018.11.046.

[35] Y. Glories, Maturité phénolique du raisin, conséquences technologiques: application aux millésimes 1991 et 1992, in: Journée Technique Du CIVB: Actes Du Colloque, 1993: pp. 56–61.

[36] N. Saint Cricq de Gaulejac, N. Vivas, Y. Glories, Maturation phénolique des raisines rouges. Relation avec la qualité des vins. Comparison des cépages Merlot et Tempranillo, Progrès Agricole et Viticole. 115 (1998) 306–318.

[37] R. Di Stefano, M.C. Cravero, Metodi per lo studio dei polifenoli dell'uva, Riv Vitic Enol 44 (1991) 37–45.

[38] R. Di Stefano, G. Maggiorotto, Antociani, acidi idrossicinnamici e flavonoli del frutto, delle foglie, dei raspi e dei tralci della vite, Riv. Vit. Enol. (1995) 51–65.

[39] P. Ribéreau-Gayon, Le dosage des anthocyanes dans le vins rouge, Bull. Soc. Chim. 9 (1965) 2649.
[40] S. Sommer, S. Cohen, Comparison of different extraction methods to predict anthocyanin concentration and color characteristics of red wines, Fermentation 4 (2018) 39, https://doi.org/10.3390/fermentation4020039.
[41] S. Río Segade, E. Soto Vázquez, E. Díaz Losada, Influence of ripeness grade on accumulation and extractability of grape skin anthocyanins in different cultivars, J. Food Compos. Anal. 21 (2008) 599–607, https://doi.org/10.1016/j.jfca.2008.04.006.
[42] R. Calvini, G. Orlandi, G. Foca, A. Ulrici, Colourgrams GUI: A graphical user-friendly interface for the analysis of large datasets of RGB images, Chemom. Intel. Lab. Syst. 196 (2020), 103915, https://doi.org/10.1016/j.chemolab.2019.103915.
[43] P. Geladi, B.R. Kowalski, Partial least-squares regression: a tutorial, Anal. Chim. Acta 185 (1986) 1–17, https://doi.org/10.1016/0003-2670(86)80028-9.
[44] S. de Jong, SIMPLS: An alternative approach to partial least squares regression, Chemom. Intel. Lab. Syst. 18 (1993) 251–263, https://doi.org/10.1016/0169-7439(93)85002-X.